Chemical Physics Letters 513 (2011) 139–144

Contents lists available at ScienceDirect

Chemical Physics Letters

journal homepage: www.elsevier.com/locate/cplett

A comparison between reduced dimensionality and mixed quantum/classical evaluations of $k(T)$ using the flux–flux correlation function formalism

Esteban Clavero, Juliana Palma *

Centro de Estudios e Investigaciones, Universidad Nacional de Quilmes, Sáenz Peña 352, B1876BXD Bernal, Argentina

ARTICLE INFO

Article history:
Received 18 June 2011
In final form 22 July 2011
Available online 26 July 2011

ABSTRACT

Rate constants for the planar $H + HD \rightarrow H_2 + D$ reaction with $J = 0$ have been calculated employing reduced dimensionality, mixed quantum/classical and full quantum computations based on the flux–flux correlation function formalism. It has been found that reduced dimensionality and mixed quantum/classical calculations afford quite similar results. This suggests that, for direct reactions occurring in the gas phase, there is no advantage in using the more involved mixed quantum/classical approach. On the other hand, the comparison between approximate and accurate results indicates that both, reduced dimensionality and mixed quantum/classical approaches, work well at medium and high temperatures. As expected, they fail at very low temperatures where tunnelling prevails.

1. Introduction

Currently, many gas phase reactions can be thoroughly studied using computational methods entirely based on first principles [1–3]. However, there is still much interest in the development and application of approximate methods. This interest stems from two main sources. First, the computational demands of calculations entirely based on first principles increases very rapidly with the number of the atoms involved. Therefore, it is important to have reliable alternatives to treat polyatomic systems. Second, through a careful analysis of the performance of approximate methods one can get deep insight into the details of the reactive process under study. For example, the comparisons between accurate and approximate results or between approximate results of different sorts may shed light on the validity of the assumptions made in non-accurate calculations.

Within the Born–Oppenheimer approximation, two basic steps are required to perform accurate computations [2]. First, electronic structure calculations are needed to determine the potential energy surface (PES) that governs the dynamics of the nuclei. Second, the quantum dynamics of the nuclei on the given PES has to be evaluated. Rate constants, as well as other parameters characterising reactivity, are extremely sensitive to the energy and configuration of the transition state (TS). But, at configurations close to the TS, electronic structure calculations become very demanding because bonds which are partially broken and partially formed need to be described. Accordingly, only high level *ab-initio* methodologies with very large basis sets can provide data of the required accuracy [2]. Then, the electronic energies have to be fitted to provide a PES that can be used in dynamical calculations. For polyatomic reactions, this fitting is also very challenging.

On the other hand, using standard techniques, the description of the quantum dynamics of the nuclei requires the use of a basis set or grid representation for each degree of freedom. Therefore, the memory needed to perform the computations roughly scales as N^f, where N is the average size of the basis set or grid, while f is the number of degrees of freedom of the system. This extremely unfavourable scaling with f prevents the accurate treatment of many polyatomic reactions of applied interests. Highly efficient methods, such as MCTDH [3], are able to treat systems larger than the standard techniques, because they require smaller values of N. In fact, this method has pushed the limit of accurate computations of $k(T)$ to twelve internal degrees of freedom several years ago [4]. However, eventually, the exponential scaling with f always poses a limit.

Reduced dimensionality (RD) [5,6] and mixed quantum/classical (mixed-Q/C) [7–9] approximations are two strategies developed to deal with quantum dynamical computations in processes that involve several atoms. They have been extensively used to study gas phase reactions, within the framework of reactive scattering theory [10–12]. Mixed-Q/C computations have also been employed in direct calculations of $k(T)$ in condensed phases [13–15]. Only very recently, mixed-Q/C computations were proposed for direct calculations of $k(T)$ in gas phase [16]. Both methods rely on the fact that not all the internal motions of a reactive system are equally important. Therefore, an accurate treatment is only given to those terms of the Hamiltonian related to the most relevant motions.

RD and mixed-Q/C methods differ in the way they treat the less important modes. In RD calculations, the variables describing these modes are fixed. Accordingly, all terms in the Hamiltonian that

* Corresponding author. Fax: +54 11 4365 7182.
E-mail address: juliana@unq.edu.ar (J. Palma).

0009-2614/$ - see front matter © 2011 Elsevier B.V. All rights reserved.
doi:10.1016/j.cplett.2011.07.069

contain derivatives for these variables vanish. In mixed-Q/C computations the less important motions are treated classically, while effective potentials are added to the quantum and classical Hamiltonians in order to allow for energy transfer between the subsystems. Briefly, it could be said that the RD approach treats the less important modes as mere spectators while the mixed-Q/C one considers them as part of a classical bath.

Thermal rate constants can be directly computed from evaluations of the flux–flux correlation function ($C_{\mathrm{ff}}(t)$), using the formalism developed by Miller and co-workers [17,18]. This formalism provides an appropriate framework for the use of RD and mixed-Q/C approximations, because the weak coupling between relevant and non-relevant degrees of freedom, assumed by these approaches, can be fulfilled to a good degree. In calculations of $C_{\mathrm{ff}}(t)$, the thermal wave packets only sample a small region of the PES, around the TS [19]. Within this region, it is not so difficult to find a coordinate system which provides a good separation. This is not always the case of reactive scattering calculations, since the nature and importance of the motions described by some coordinates change when going from the asymptotic regions to the transition state. Thus, for example, coordinates describing translational and rotational motions, at the asymptotic parts of the PES, describe quantized vibrations at the strong interaction region. On the other hand, direct evaluations of $k(T)$ require shorter propagation times than those typically employed in reactive scattering calculations [20]. Therefore, the non-important modes have less time to interact with the relevant modes and modify their dynamics.

In spite of the similarities there are also significant differences between RD and mixed-Q/C calculations. Basically, it could be said that RD calculations are somewhat simpler or less-involved than the corresponding mixed-Q/C ones. While an RD evaluation of $C_{\mathrm{ff}}(t)$ requires a single propagation of the thermal wave packets, the mixed Q/C approach requires the calculation of many trajectories [15]. Besides, mixed-Q/C propagation schemes need significantly smaller integration steps than the full quantum ones, in order to keep the energy of the combined system constant. Altogether, these two facts make the mixed-Q/C computations more time consuming than the RD ones. But there is an even more important feature that differentiates these two approaches. Mixed-Q/C calculations need a full-dimensional PES, while RD computations can be performed with a RD-PES. This is an extremely simplifying feature that, as Kerkeni and Clary have demonstrated, allows for good estimations of $k(T)$ in polyatomic reactions, at a reasonable computational cost [21–23]. Because of the reduced size of the potential that needs to be developed, RD surfaces can be evaluated at higher levels of theory than full-D surfaces. This often increases the accuracy of the calculated rate constants. It is, therefore, interesting to know whether the more-involved mixed-Q/C approach provides different results than the RD approach. Otherwise one should prefer employing RD calculations.

In this Letter we compare the results of RD and mixed-Q/C direct computations of $k(T)$. Mainly, we want to know if the estimates obtained with the two approaches are similar or not. If not, we want to establish which of the two methods provides the best estimate. In order to do so, we also perform comparisons with full quantum (full-QM) results. The reactive system used to answer these questions is a planar version of the $H + HD \rightarrow H_2 + D$ reaction with $J = 0$. We should note that, with the same computational effort, we could have done the calculations in 3D since both, the planar and 3D $J = 0$ Hamiltonians have three internal degrees of freedom. However, the use of the planar Hamiltonian allows a closer comparison between the methods. In the plane, the operator that describes the bending motion at the TS nicely transforms into its classical counterpart, when the procedure developed by Ratner et al. [24] is applied. This does not hold for the operator that describes the bending motion in 3D. In this case, an *ad-hoc* classical Hamiltonian would have to be introduced. Such a procedure, which would add a putative source of difference between RD and mixed-Q/C results, would clearly interfere in the comparison.

The $H + H_2 \rightarrow H_2 + H$ reaction is the simplest and the most studied system [25]. Because of this, it is usually employed to test approximated methodologies. In this work we use an isotopic variant of it, in order to differentiate between the two different product channels. The methods we are testing are aimed to treat reactions of the general type $A + BC \rightarrow AB + C$, where only one product channel is relevant, or where the different product channels can be treated independently. In the next section we describe the methodology employed to perform the computations. Then, in Section 3, we present and discuss the results. Section 4 finishes this letter highlighting the main conclusions of the work.

2. Methodology

The full quantum Hamiltonian for the planar $H + HD \rightarrow H_2 + D$ reaction with $J = 0$ can be written as

$$\widehat{H} = \widehat{K}_{\mathrm{q}} + \widehat{K}_{\mathrm{b}} + V. \tag{1}$$

Here $\widehat{K}_{\mathrm{q}}$ is the kinetic energy operator that describes the symmetric and asymmetric stretching vibrations at the TS, while $\widehat{K}_{\mathrm{b}}$ describes the corresponding bending motion. The last term of Eq. (1) accounts for the potential energy of the system.

The operator $\widehat{K}_{\mathrm{q}}$ was expressed in hyperspherical coordinates ρ and δ defined as

$$\rho = \sqrt{\mu_R R^2 + \mu_r r^2},$$
$$\delta = \arctan\left(\frac{\sqrt{\mu_r} r}{\sqrt{\mu_R} R}\right),$$

where r and R are the lengths of the Jacobi vectors depicted in Figure 1 while μ_r and μ_R are the corresponding reduced masses,

$$\mu_r = m_H m_D/(m_H + m_D),$$
$$\mu_R = m_H(m_H + m_D)/(2m_H + m_D).$$

In the last two equations, m_H and m_D are the masses of isotopes protium and deuterium, respectively.

Employing atomic units, the operator $\widehat{K}_{\mathrm{q}}$ takes the form

$$\widehat{K}_{\mathrm{q}} = -\frac{1}{2}\left(\frac{\partial^2}{\partial\rho^2} + \frac{1}{\rho^2}\frac{\partial^2}{\partial\delta^2}\right) - \frac{1}{8}\left(\frac{1}{I_\alpha(\rho,\delta)} + \frac{1}{I_\beta(\rho)}\right), \tag{2}$$

where $I_\alpha = \rho^2\sin^2(\delta)\cos^2(\delta)$ and $I_\beta = \rho^2$. The last two terms of Eq. (2) appear when the wave function is scaled so that the volume element is just $d\rho d\delta$. Finally, the kinetic energy operator for the bending vibration takes the form

$$\widehat{K}_{\mathrm{b}} = -\frac{1}{I_\alpha(\rho,\delta)}\frac{\partial^2}{\partial\alpha^2}, \tag{3}$$

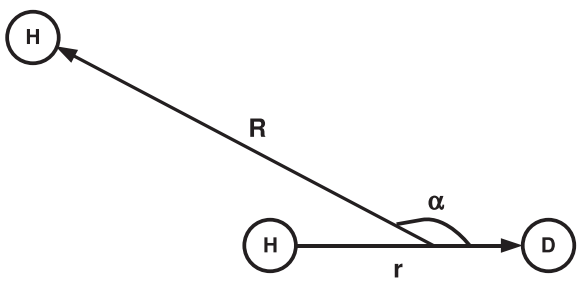

Figure 1. Jacobi coordinates employed in the definition of the hyperspherical coordinates ρ and δ. The angle α, that describes the bending vibration at the transition state, is also shown.

where α is the angle between vectors r and R, as shown in Figure 1. Curvilinear coordinates as the ones employed here, tend to minimise the correlation between variables. Therefore they are appropriate for implementing approximations like the mixed-Q/C one, which relies on the validity of the time-dependent-self-consistent-field approach [24].

Reduced dimensionality computations were performed by fixing the bending angle to its transition state value ($\alpha^{\#} = \pi$). Accordingly, the RD Hamiltonian reads

$$\widehat{H}^{RD} = \widehat{K}_q + V(\rho, \delta, \alpha^{\#}). \tag{4}$$

The mixed-Q/C model was defined so that $\widehat{K}_q$ belongs to the quantum subsystem while $\widehat{K}_b$ belongs to the classical one. The potential energy terms for the quantum and classical subsystems were defined as

$$V_q(\rho, \delta) = V(\rho, \delta, \alpha^{\#}),$$
$$V_b(\alpha) = V(\rho^{\#}, \delta^{\#}, \alpha) - V(\rho^{\#}, \delta^{\#}, \alpha^{\#}),$$

where $\rho^{\#}$ and $\delta^{\#}$ are the values taken by these variables at the transition state. Therefore, the coupling potential is

$$V_{coup}(\rho, \delta, \alpha) = V(\rho, \delta, \alpha) - (V_q(\rho, \delta) + V_b(\alpha)). \tag{5}$$

These definitions produce relatively small values of V_{coup} in the region sampled by the thermal wave packets and this helps to improve the quality of the quantum/classical separation.

To obtain the effective Hamiltonians to be used in the quantum/classical propagations we followed the procedure developed by Ratner et al. [24]. The solution of the full-dimensional time-dependent Schrödinger equation is proposed to have the form $\psi(\rho,\delta,\alpha,t) = \phi_q(\rho,\delta,t)\phi_b(\alpha,t)$. Besides it is assumed that $\phi_b(\alpha,t) = a(\alpha,t)e^{-iS(\alpha,t)t/\hbar}$, with $a(\alpha,t)$ being an approximate delta function centred at $\alpha(t)$. By introducing this ansatz in the Hamiltonian of Eq. (1) and then taking the limit $\hbar \to 0$, the following effective Hamiltonians are obtained, provided that the dependence of $\widehat{K}_b$ with ρ and δ is ignored [26],

$$\widehat{H}_q^{eff} = \widehat{K}_q + V_q(\rho, \delta) + V_{coup}(\rho, \delta, \alpha(t)), \tag{6}$$

$$\widehat{H}_b^{eff} = \frac{p_\alpha^2}{2\bar{I}_\alpha} + V_b(\alpha) + \langle V_{coup}(\rho, \delta, \alpha)\rangle_{\rho,\delta}. \tag{7}$$

In these equations, the symbol $\langle \dots \rangle_{\rho,\delta}$ indicates averaging over the quantum wave function while $\bar{I}_\alpha$ is the value given to $I_\alpha(\rho,\delta)$ when its dependence with the hyperspherical variables is ignored. We tested two different ways of assigning $\bar{I}_\alpha$. In the simplest approach, named QC–TS, we set $\bar{I}_\alpha = I_\alpha(\rho^{\#}, \delta^{\#})$. Alternatively, we used $\bar{I}_\alpha = \langle I_\alpha(\rho,\delta)\rangle_{\rho,\delta}^{t=0}$, where the superscript $t = 0$ indicates that the integral is evaluated using the initial thermal wave packet. We named this approach as QC–AVE. We found that the two approaches give very similar results, with the QC–TS values always below the QC–AVE ones by 1–4%. Since, in turn, the QC–AVE values were always closer to the full-QM results, we will only present and discuss in section 3 the mixed-Q/C results obtained with the QC–AVE approach.

During mixed-Q/C calculations, the state of the quantum subsystem was propagated by numerical integration of the time-dependent Schrödinger equation, corresponding to the effective Hamiltonian of Eq. (6). The state of the classical subsystem was propagated using the classical equations of motion, corresponding to the Hamiltonian of Eq. (7). This propagation scheme is the one usually employed in mixed-Q/C computations. It conserves the energy of the composed system, in the limit of infinitely-small time steps. Thus, the quality of the trajectories can be assessed by analysing the variations of the total energy.

Full quantum direct evaluations of $k(T)$ were based on the expression proposed by Miller et al. [18],

$$Q_r(T)k(T) = \int_0^\infty C_{ff}(t)dt, \tag{8}$$

where $Q_r(T)$ is the reactant partition function per unit volume, while the flux–flux correlation function is given by,

$$C_{ff}(t) = \mathrm{Tr}\left[\widehat{F}(\beta)e^{i\widehat{H}t/\hbar}\widehat{F}e^{-i\widehat{H}t/\hbar}\right]. \tag{9}$$

Here $\widehat{F} = [\widehat{H}, h]$ is the flux operator, h is the Heaviside step function, $\beta = (kT)^{-1}$ and $\widehat{F}(\beta)$ is the Boltzmannized flux operator

$$\widehat{F}(\beta) = e^{-\beta\widehat{H}/2}\widehat{F}e^{-\beta\widehat{H}/2}. \tag{10}$$

By introducing the spectral decomposition of $\widehat{F}(\beta)$ in Eq. (9), a numerically convenient expression to evaluate $C_{ff}(t)$ is obtained [15],

$$C_{ff}(t) = \sum_{j=1}^{N_f} f_j \langle u_j(t)|\widehat{F}|u_j(t)\rangle. \tag{11}$$

Here f_j and $|u_j\rangle$ are the eigenvalues and eigenfunctions of $\widehat{F}(\beta)$, respectively, N_f is the number of eigenfunctions of $\widehat{F}(\beta)$ with non-negligible eigenvalues, while the $|u_j(t)\rangle$'s are the time-evolved $|u_j\rangle$,

$$|u_j(t)\rangle = e^{-i\widehat{H}t/\hbar}|u_j\rangle. \tag{12}$$

The eigenfunctions $|u_j\rangle$ were obtained by diagonalizing the representation of $\widehat{F}(\beta)$ in the basis set of eigenfunctions of $\widehat{H}$. In turn, the eigenfunctions of $\widehat{H}$ were obtained by diagonalizing the representation of this operator in a direct-product particle-in-a-box DVR basis set, for the variables ρ, δ and α. The calculation of the eigenfunctions of $\widehat{F}(\beta)$ only included eigenfunctions of $\widehat{H}$ with eigenvalues smaller than E_{lim}. Similarly, in the summation of Eq. (11) we only considered eigenfunctions $|u_j\rangle$ whose eigenvalues fulfil $|f_j/f_1| \geqslant F_{min}$.

Reduced dimensionality and mixed-Q/C estimations of $C_{ff}(t)$ were obtained from

$$C_{ff}(t) \approx Q_b^{\#} C_{ff}^{APP}(t), \tag{13}$$

where $Q_b^{\#}$ is the partition function of the modes that receive an approximate treatment, while APP = RD or QC indicates which of the two approaches is being employed to estimate the flux–flux correlation function. Eq. (13) would hold exactly if the separation between important and non-important modes were exact.

The RD flux–flux correlation function, C_{ff}^{RD}, was calculated using an expression similar to Eq. (11), with the only difference that the flux operator, and therefore thermal-flux eigenfunctions, corresponded to the RD Hamiltonian of Eq. (4) instead of the full-QM one of Eq. (1). The procedure followed to obtain and propagate the RD thermal-flux eigenfunctions was similar to the one employed in full-QM computations. The mixed-Q/C flux–flux correlation function was evaluated with the formula proposed by Wang et al. [15]

$$C_{ff}^{QC} = Q_b^{\#}\frac{1}{N_{traj}}\sum_{n=1}^{N_{traj}}\sum_{j=1}^{N_f} f_{q,j}\left\langle u_{q,j}^{n}(t)\middle|\widehat{F}_q\middle|u_{q,j}^{n}(t)\right\rangle_{\rho,\delta}. \tag{14}$$

In this expression N_{traj} is the number of mixed-Q/C trajectories, $\widehat{F}_q$ is the flux operator corresponding to the effective quantum Hamiltonian of Eq. (6), while $f_{q,j}$ and $|u_{q,j}(t)\rangle$ are the eigenvalues and time-evolved eigenfunctions of $\widehat{F}_q(\beta)$. The superscript n denotes the trajectory being used to evaluate $|u_{q,j}^{n}(t)\rangle$. The trajectories of Eq. (14) were initiated by selecting the classical coordinate and momentum at random from their classical distribution probabilities, while the quantum subsystem was set at a given eigenstate of $\widehat{F}_q(\beta)$. The trajectories were integrated using the PICKABACK algorithm, which is especially suited for mixed-Q/C propagations

Table 1
Parameters employed in RD, mixed-Q/C and full-QM computations.

	QM	RD	QC
V_{max}/kcal mol^{-1}	65.0	65.0	65.0
E_{lim}/kcal mol^{-1}	30.0	40.0	40.0
F_{min}	1.0e−2	1.0e−3	1.0e−3
δ_{min}	0.08	0.08	0.08
δ_{max}	0.96	0.96	0.96
N_δ	30	50	50
ρ_{min}/a.u.	70.0	70.0	70.0
ρ_{max}/a.u.	290.0	290.0	290.0
N_ρ	30	60	60
α_{min}/rad	1.02	–	–
α_{max}/rad	4.36	–	–
N_α	20	–	–

[20]. The procedure used to obtain the eigenvalues and eigenfunctions of $\widehat{F}_q(\beta)$ was the same as the one employed in RD calculations. Following Wang et al. [15], the coupling potential $V_{coup}(\rho, \delta, \alpha)$ was not included in $\widehat{H}_q$ at the time of calculating the eigenvalues and eigenfunctions of $\widehat{F}_q(\beta)$.

The values of the parameters defined in this section, that were used to obtain the results presented in the next section, are shown in Table 1. Other parameters, which have not been explicitly mentioned before, but are needed to reproduce the calculations, are also included in the Table. These are: the sizes of the primitive DVR grids (N_δ, N_ρ and N_α), the minimum and maximum values taken by each coordinate ([δ_{min}:δ_{max}], [ρ_{min}:ρ_{max}] and [α_{min}:α_{max}]) and the maximum value of the potential energy, for the DVR points included in the evaluation of the Hamiltonian matrix (V_{max}). All the computations were performed using the BKMP2 surface of Boothroyd et al. [27,28].

Approximately 100 mixed-Q/C trajectories for each temperature value are needed to compute thermal rate constants with negligible statistical uncertainty. This means that the time required by a mixed-Q/C evaluation of $k(T)$ is, at least, two orders of magnitude larger than that of a RD computation. Besides, one must consider that a single quantum/classical trajectory takes significantly longer than a RD trajectory. This is mainly due to the shorter time-steps required by the mixed-Q/C propagation. In our implementation, we used 5.0×10^{-3} fs for mixed-Q/C trajectories and 1.0×10^{-1} fs for the RD ones. With this setting, the ratio between the CPU times required by a mixed-Q/C trajectory and a RD one was about 50. We note, however, that this ratio can be sensitive to the system under study.

3. Results and discussion

Combining Eq. (8) with Eq. (13), the following expression is obtained for the approximated $k(T)$s

$$Q_r(T)k^{APP}(T) = Q_b^{\#}\int_0^\infty C_{ff}^{APP}(t)dt. \quad (15)$$

The comparison of this expression with Eq. (8) shows that there are two factors determining the agreement between approximated and full quantum rate constants. One is a dynamical factor contained in the integral $\int_0^\infty C_{ff}^{APP}(t)dt$. The other one is a thermodynamical factor corresponding to the partition function of the modes treated approximately. However, only the former is relevant in the comparison between RD and mixed-Q/C calculations. Accordingly, we will use it henceforth to evaluate the agreement between the two approaches.

Mixed-Q/C and RD values of the integral $\int_0^\infty C_{ff}^{APP}(t)dt$ are shown in Figures 2 and 3, for the lowest (200 K) and the highest (1000 K) temperatures considered in this work, respectively. We also present there the results of a few individual mixed-Q/C trajectories, selected at random, in order to illustrate their typical behaviour. It can be noted that computations done at 1000 K reach their asymptotic values faster than computations done at 200 K. Another difference is that the results of individual trajectories are much more spread out at 200 K than at 1000 K. In fact, these two features are related to each other. The thermal wave packets move faster at higher temperatures. Accordingly they leave the strong interaction region in a shorter time. But, for the same reason, the influence of the classical subsystem onto the quantum one is smaller, producing trajectories which look pretty similar to each other.

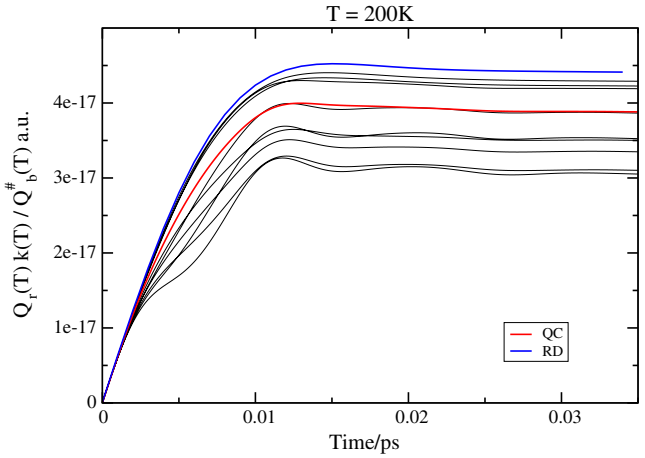

Figure 2. Values of the integral $\int_0^\infty C_{ff}^{APP}(t)$ at $T = 200$ K for APP = RD (blue) and APP = QC (red). The results of ten individual mixed-Q/C trajectories are also presented (black). (For interpretation of the references in colour in this figure legend, the reader is referred to the web version of this article.)

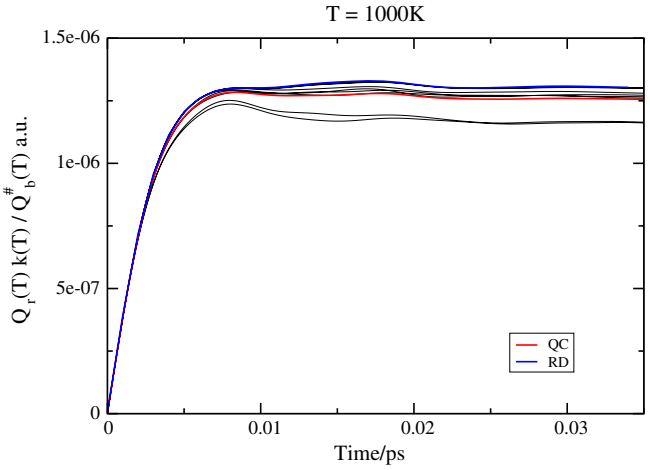

Figure 3. Values of the integral $\int_0^\infty C_{ff}^{APP}(t)$ at $T = 1000$ K for APP = RD (blue) and APP = QC (red). The results of ten individual mixed-Q/C trajectories are also presented (black). (For interpretation of the references in colour in this figure legend, the reader is referred to the web version of this article.)

Figures 2 and 3 show that mixed-Q/C results are below the RD ones, and that the difference between them is larger at the lowest temperature. A more quantitative comparison can be done using the data of Table 2. There, we present the results obtained at five different temperatures between 200 K and 1000 K. The data in the Table confirm the trends observed in Figures 2 and 3. The fact that the agreement between RD and mixed-Q/C results becomes better at higher temperatures is not surprising. It can be understood with the same reasoning discussed in the previous paragraph. At higher temperatures the thermal wave packets move faster and therefore have less time to interact with the classical

Table 2
Converged values of $\int_0^\infty C_{ff}^{APP}(t)dt$ for APP = RD and QC. The statistical uncertainty of the QC results is given within parenthesis.

T/K	RD	QC
200	4.41e−17	3.88(0.05)e−17
400	8.77e−11	7.87(0.03)e−11
600	1.60e−08	1.49(0.02)e−08
800	2.41e−07	2.26(0.02)e−07
1000	1.30e−06	1.26(0.01)e−06

subsystem. In the limit of very high temperatures the two approaches should agree, within their statistical and numerical uncertainties. On the other hand, we have no explanation for the fact that mixed-Q/C results underestimate the RD ones. Moreover, we do not know whether this is a general feature or just one unique to the present reaction. It would be necessary to study several reactions, involving different mass combinations and potential energy surfaces, in order to address that question. Nevertheless, we should note that the differences are small. In the worst case, found at 200 K, the mixed-Q/C value underestimate the RD one by just ≈12%.

Finally, in order to be able to compare with full-QM calculations, the values of the integral $\int_0^\infty C_{ff}^{APP}(t)dt$, computed at different temperatures, were multiplied by the partition function of the bending mode. The partition functions were calculated using the eigenvalues of the one-dimensional Hamiltonian, corresponding to the bending vibration at the transition state. Similar results are obtained when the partition functions are approximated using the harmonic frequency of that mode. The results are presented in Figure 4. The agreement between approximated and full-QM results is very good at the higher temperatures, but deteriorates at lower temperatures. At 1000 K, the RD results underestimate the full-QM ones by just 6.6%, while at 400 K this error increases to 18.1%. At 200 K, where the reaction occurs mainly by tunnelling, the approximated values fail to give a good estimate of the full-QM results. This failure gives a strong indication of the limitations of the models employed here, to deal with such situations.

At this point, we should note that the PES employed in the RD computations did not include a zero point energy correction for the bending mode. Instead, they were performed on the bare electronic PES. In this sense, our computations are similar to RD scattering calculations that employ a simple energy shifting approximation. The evidence collected so far, from reactive scattering calculations [10], indicates that the adiabatic correction provides more accurate results than the energy shifting approximation. Therefore, the comparison between RD and full-QM computations presented here could probably be improved by adding the zero point energy of the bending mode to the electronic PES.

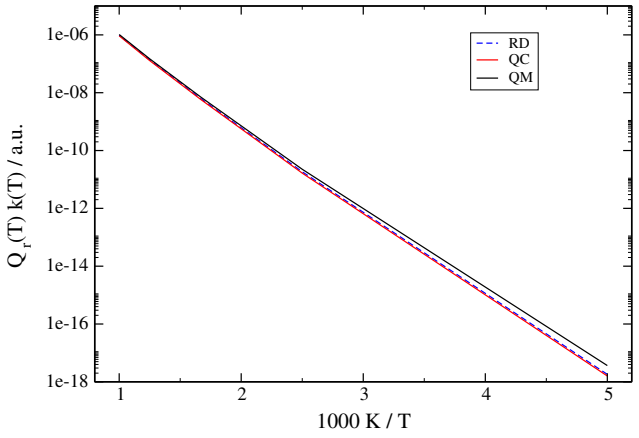

Figure 4. Converged values of $Q_r(T)k(T)$ for $J = 0$ as a function of T. Full-QM (full-line, black), RD (dashed-line, blue); mixed-Q/C (full-line, red). (For interpretation of the references in colour in this figure legend, the reader is referred to the web version of this article.)

The $H + HD \rightarrow H_2 + D$ reaction with $J = 0$ has only three degrees of freedom, while the method we are testing is aimed at dealing with larger systems. Thus, one important question immediately arises. How much of what we have learned in this work can be extrapolated to more complex cases? A conclusive answer to this question requires the comparison between RD and mixed-Q/C results, and between them and full-QM results, for a significant number of polyatomic reactions. However, for the time being, some tentative answers can be given by exploring the causes for the agreement or disagreement between the results obtained through different approaches. The fact that RD and mixed-Q/C calculations produce nearly the same results is related to the short time it takes for the flux–flux correlation function to converge to zero. Thus, one can expect that this finding remains true for all direct abstraction reactions taking place in gas phase. For such systems, the much simpler RD approach should be preferred to the mixed-Q/C approach, because it provides the same (or perhaps higher) accuracy with less computational effort. This situation is completely different from that found in the study of condensed phase reactions [13,14], where the bath modes play a far more important role [29].

On the other hand, the poor agreement between full-QM and approximated results found at 200 K indicates that, where tunnelling prevails, the three degrees of freedom of the system are required to account for reactivity. Accordingly, it is not appropriate considering the bending vibration as a non-important mode. The relevance of these low-frequency bending vibrations has been highlighted in a recent study, in which the performance of RD models applied to the $H + CH_4$ reaction was analysed [30]. For a small system as the one treated in this work, the only solution is to perform full-QM calculations. However, when dealing with larger systems, RD models with three or four degrees of freedom could be employed. These models could explicitly include the low-frequency bending vibrations of the TS in their Hamiltonians. Today, three and even four dimensional quantum dynamical computations are readily affordable, provided that an appropriate PES is available. We note, however, that computing accurate surfaces in four dimensions can be a challenge. Surely, this is one of the challenges to overcome in order to implement RD direct computations of $k(T)$ with more than two dimensions.

4. Conclusions

We have calculated mixed quantum/classical (mixed-Q/C), reduced dimensionality (RD) and full quantum rate constants for the planar $H + HD \rightarrow H_2 + D$ reaction with $J = 0$, using the formalism of the flux–flux correlation function. The comparison between RD and mixed-Q/C results suggests that there is no advantage in using the more involved mixed-Q/C approach. However, since the system analysed in this letter is relatively small, additional tests should be made on larger systems, such as $H + CH_4$, in order to confirm this suggestion. On the other hand, the comparison between approximated and accurate results shows that, while both approaches work well at medium and high temperatures, they fail to reproduce full quantum results at very-low temperatures where tunnelling prevails. This failure was attributed to the limitations of the RD and mixed-Q/C models studied here. Both models treat the bending vibration of the TS approximately. This vibration is required to properly describe the tunnelling regime. When dealing with larger and more complicated reactions this problem could be mitigated by defining larger RD Hamiltonians which include such a

vibration. Also, the use of a zero point energy correction for the modes not considered in the RD model could help to improve the performance of the approach.

Aknowledgements

This work was supported CONICET and the Universidad Nacional de Quilmes. EC thanks to CONICET for his postdoctoral fellowship. Thanks are given to Santiago De Rosa for the useful suggestions and careful reading of this manuscript.

References

[1] W. Hu, G.C. Schatz, J. Chem. Phys. 125 (2006) 132301.
[2] D.C. Clary, Science 321 (2008) 789.
[3] F. Huarte-Larrañaga, U. Manthe, Multidimensional Quantum Dynamics: MCTDH Theory and Applications, Wiley, 2009.
[4] T. Wu, H. Werner, U. Manthe, Science 306 (2004) 2227.
[5] J.M. Bowman, J. Phys. Chem. 95 (1991) 4960.
[6] D.C. Clary, J. Phys. Chem. 98 (1994) 10678.
[7] L. Wang, A.B. McCoy, Phys. Chem. Chem. Phys. 1 (1999) 1227.
[8] L. Wang, W.J. Meurer, A.B. McCoy, J. Chem. Phys. 113 (2000) 10605.
[9] L. Wang, A.B. McCoy, J. Chem. Phys. 119 (2003) 1996.
[10] J.M. Bowman, Theor. Chim. Acta 108 (2002) 125.
[11] D. Zhang, M. Yang, M. Collins, S.-Y. Lee, in: A. Lagana, G. Lendvay (Eds.), Theory of Chemical Reaction Dynamics, NATO Science Series, vol. 45, Springer Netherlands, 2005, pp. 279–303.
[12] G. Pierdominici-Sottile, S.F. Alberti, J. Palma, in: J.R. Sabin, E. Brändas (Eds.), Combining Quantum Mechanics and Molecular Mechanics. Some Recent Progresses in QM/MM Methods, Advances in Quantum Chemistry, vol. 59, Academic Press, 2010, p. 247.
[13] G. Wahnstrom, B. Carmeli, H. Metiu, J. Chem. Phys. 88 (1988) 2478.
[14] G. Wahnstrom, H. Metiu, J. Phys. Chem. 92 (1988) 3240.
[15] H. Wang, X. Sun, W.H. Miller, J. Chem. Phys. 108 (1998) 9726.
[16] J. Palma, J. Chem. Phys. 130 (2009) 124119.
[17] W.H. Miller, J. Phys. Chem. 102 (1998) 793.
[18] W.H. Miller, S.D. Schwartz, J.W. Tromp, J. Chem. Phys. 79 (1983) 4889.
[19] F. Huarte-Larrañaga, U. Manthe, Z. Phys. Chem. 221 (2007) 171.
[20] F.A. Bornemann, P. Nettesheim, C. Schutte, J. Chem. Phys. 105 (1996) 1074.
[21] B. Kerkeni, D.C. Clary, J. Phys. Chem. A 107 (2003) 10851.
[22] B. Kerkeni, D.C. Clary, J. Phys. Chem. A 108 (2004) 8966.
[23] B. Kerkeni, D.C. Clary, J. Chem. Phys. 123 (2005) 064305.
[24] R.B. Gerber, V. Buch, M.A. Ratner, J. Chem. Phys. 77 (1982) 3022.
[25] F.J. Aoiz, Int. Rev. Phys. Chem. 24 (2005) 119. 72.
[26] E. Clavero, J. Palma, Int. J. Quant. Chem. 111 (2011) 1773.
[27] A.I. Boothroyd, W.J. Keogh, P.G. Martin, M.R. Peterson, J. Chem. Phys. 95 (1991) 4343.
[28] A.I. Boothroyd, W.J. Keogh, P.G. Martin, M.R. Peterson, J. Chem. Phys. 104 (1996) 7139.
[29] D. Laria, G. Ciccotti, M. Ferrario, R. Kapral, J. Chem. Phys. 97 (1992) 378.
[30] G. Schiffel, U. Manthe, J. Chem. Phys. 132 (2010) 084103.